Anthropogenic sulfate aerosol and the southward shift of tropical precipitation in the late 20th century

Yen-Ting Hwang,[1] Dargan M. W. Frierson,[1] and Sarah M. Kang[2]

Received 5 February 2013; revised 16 April 2013; accepted 22 April 2013.

[1] In this paper, we demonstrate a global scale southward shift of the tropical rain belt during the latter half of the 20th century in observations and global climate models (GCMs). In rain gauge data, the southward shift maximizes in the 1980s and is associated with signals in Africa, Asia, and South America. A southward shift exists at a similar time in nearly all CMIP3 and CMIP5 historical simulations, and occurs on both land and ocean, although in most models the shifts are significantly less than in observations. Utilizing a theoretical framework based on atmospheric energetics, we perform an attribution of the zonal mean southward shift of precipitation across a large suite of CMIP3 and CMIP5 GCMs. Our results suggest that anthropogenic aerosol cooling of the Northern Hemisphere is the primary cause of the consistent southward shift across GCMs, although other processes affecting the atmospheric energy budget also contribute to the model-to-model spread.
Citation: Hwang, Y.-T., D. M. W. Frierson, and S. M. Kang (2013), Anthropogenic sulfate aerosol and the southward shift of tropical precipitation in the late 20th century, *Geophys. Res. Lett.*, *40*, doi:10.1002/grl.50502.

1. Introduction

[2] The steady decrease of rainfall in the Sahel, beginning in the 1950s and peaking with a pronounced minimum in rainfall in the early 1980s, is perhaps the most striking precipitation change in the 20th century observational record [*Nicholson*, 1993; *Dai et al*., 2004]. Sea surface temperature (SST) patterns are often implicated in changes in tropical precipitation. *Folland et al*. [1986] linked this drought with the relative changes in sea surface temperature between the hemispheres that were observed worldwide. *Giannini et al*. [2003] and *Zhang and Delworth* [2006] demonstrated the responses of rainfall in the Sahel to ocean forcing through single-model experiments. Tropical precipitation over Asia can also be affected by interhemispheric SST patterns. *Chung and Ramanathan* [2006] demonstrated the effect of north-south SST gradients in the tropical Indian Ocean on the Asian summer monsoon.

[3] In this paper, we examine global precipitation changes in the late 20th century in observations and global climate model (GCM) simulations from the Coupled Model Intercomparison Project Phase 3 and Phase 5 (CMIP3 and CMIP5) and look for the causes of the southward precipitation shift. Local SSTs have a direct link with tropical rainfall; however, they may not be the root cause. *Friedman et al*. [2013] analyzed the temperature contrast between the Northern Hemisphere (NH) and Southern Hemisphere (SH) in various data sets and reported a drop in the NH minus SH temperature during 1960s to 1980s, followed by a steady increase. An increase of sulfate aerosol concentration, multidecadal ocean variability, and discrete cooling events in the Northern Hemisphere (NH) oceans have all been proposed to explain the observed SST variability [*Tett et al*., 2002; *Knight et al*., 2005; *Thompson et al*., 2010].

[4] We perform an attribution analysis of the zonal mean tropical precipitation changes in GCMs using a method based on energetic constraints [*Frierson and Hwang*, 2012; *Hwang and Frierson*, 2013]. The energetic framework, described in section 3, essentially posits that the tropical rain belt is drawn toward the hemisphere with more heating. By analyzing factors contributing to the hemispheric asymmetry of heating, we conclude in section 4 that aerosol forcings are the primary cause of the late 20th century shift in GCMs. Other factors, such as longwave cloud effects, the water vapor greenhouse effect, and ocean heat uptake and circulation changes, also contribute, but their effects vary among models.

2. The Global-Scale Southward Shift of Tropical Rainfall

[5] We examine precipitation in the Global Historical Climatology Network (GHCN) gridded products [*Peterson and Vose*, 1997], which takes into account precipitation data from stations throughout the world. Drying of the northern side and wetting of southern side of the tropical rain belt from the late 1960s to the 1980s is seen in its zonal mean (Figure 1a). Negative anomalies of over 10 cm/yr in the zonal mean just north of the equator in the early 1950s become positive anomalies of 10 cm/yr by the mid 1980s. South of the equator, the changes are less prominent than those in the NH but are generally of opposite sign to the changes north of the equator.

[6] The drying of the NH tropics during 1971–1990 is most significant in the Sahel region but it is also observed in South America and South Asia over limited regions that have station data available (Figure 2a). A moistening south of the equator around northeast Brazil and the African Great Lakes region is also observed (Figure 2a). An independent precipitation data set that has complete spatial coverage over land and ocean, the 20th Century Reanalysis (20CR)

Additional supporting information may be found in the online version of this article

[1]Department of Atmospheric Sciences, University of Washington, Seattle, Washington, USA.
[2]School of Urban and Environmental Engineering, Ulsan National Institute of Science and Technology, Ulsan, South Korea.

Corresponding author: Y.-T. Hwang, Department of Atmospheric Sciences, University of Washington, USA. (yting@atmos.washington.edu)

0094-8276/13/10.1002/grl.50502

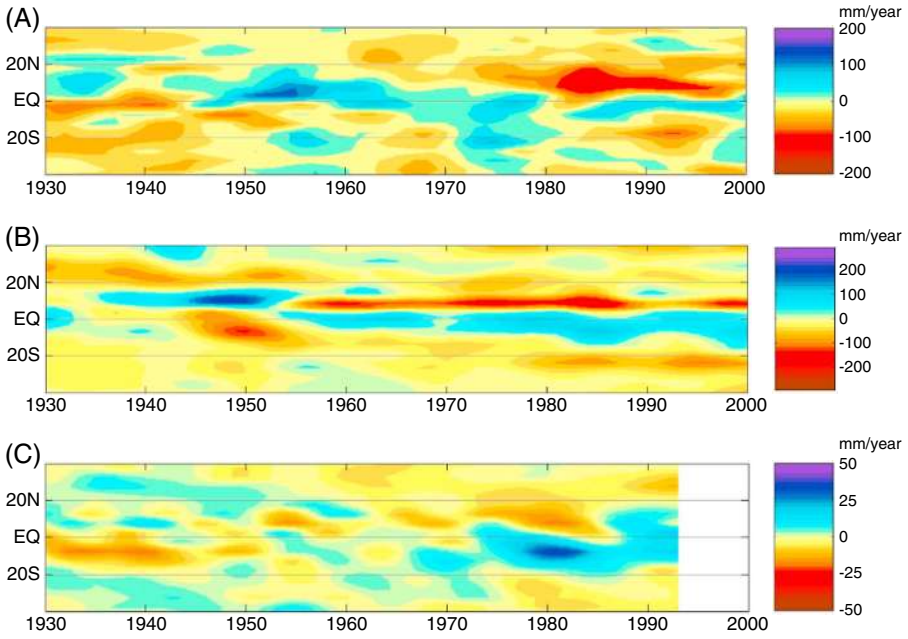

Figure 1. Time series of zonal mean precipitation anomaly. Zonal mean precipitation anomaly (relative to the 20th century mean) based on (a) the Global Historical Climatology Network (GHCN) gridded products, (b) the 20th century reanalysis project (20CR), and (c) the ensemble mean of the 20th century climate simulations from 14 GCMs in CMIP3 and 12 GCMs from CMIP5. Values are smoothed with the 13-point filter to remove fluctuations of less than decadal time scales [as in *Solomon et al*., 2007].

[*Compo et al*., 2011], shows a more significant southward shift (Figures 1b and 2d). In 20CR, the shift occurs over both land and ocean (Figure 2b) but has discrepancies compared with the rain gauge data in terms of timing, magnitude, and spatial pattern. It is unclear whether this is in part due to the addition of oceanic data points or is primarily due to inadequacies of the reanalysis product. In the Supplementary Materials, we show that 20CR captures the primary variability patterns of precipitation in recent decades and therefore is a useful secondary confirmation of a southward shift during the late 20th century. In addition to GHCN and 20CR, we also examine Global Precipitation Climatology Centre (GPCC) and Climate Research Unit (CRU) data [*Schneider et al*., 2013; *Mitchell and Jones*, 2005], which are both based on quality-controlled station data but use different algorithm to interpret the data to gridded product covering all land area. Both GPCC and CRU data demonstrate the southward shift of rainfall, although spatial patterns differ over the area without continuous record of station data (Supplementary Figures S3 and S4).

[7] Do GCMs simulate the observed southward shift of rainfall seen in GHCN and 20CR data? We analyze historical simulations, experiments that consider both natural and anthropogenic forcings to simulate the climate during the 20th century, from all CMIP3 and CMIP5 models (listed in Supplementary Figure S5). Note that we use a simple index to define precipitation shift (changes in precipitation from equator to 20°N minus equator to 20°S), as detailed spatial patterns of the shift are data set dependent and most GCMs have the so-called double rainband problem in climatology [*Lin*, 2007; *Hwang and Frierson*, 2013], making the shift harder to define. By focusing on the simple index that capture large-scale patterns, we find that most GCMs simulate some degree of the southward shift, although all but a few underestimate it by at least a factor of 2 (Figure 3a, the shifts of each GCM are shown in the y axis). In the multimodel time series (Figure 1c), the anomalously dry NH tropics is most prominent in the years around 1980, when the SH tropics was anomalously moist. The multimodel mean anomaly map (Figure 2c) shows that the modeled shift is remarkably zonally symmetric, with the exception of the west Pacific and Southeast Asia.

3. The Global Energetic Framework and the Attribution Analysis

[8] In this section, we investigate the cause of the robust southward shift across GCMs with a theoretical framework based on energetic constraints of the system [*Frierson and Hwang*, 2012; *Kang et al*., 2008; *Kang et al*., 2009]. The Hadley circulation is the foundation of this global energetic framework. While it transports energy poleward in the upper branch, its lower branch also converges moisture toward the tropical rain belt. The Hadley circulation creates a strong link between the hemispheric heating asymmetry and location of the tropical rain belt. For example, when cooling is imposed in the NH, the northern Hadley cell strengthens to transport energy northward and keeps the tropospheric temperature flat within the tropics. At the same time, moisture transport in the lower branch shifts the tropical rain belt southward. Forcings within the tropics are not necessary to cause shifts in the tropical rain belt. High-latitude forcings cause shifts in the tropical rain belt as well, with southward shifts in response to increases in NH sea ice [*Chiang and Bitz*, 2005] or reductions in the thermohaline circulation [*Zhang and Delworth*, 2005]. Our theoretical framework predicts that the tropical rain belt will shift away from the hemisphere with more cooling (or toward the hemisphere

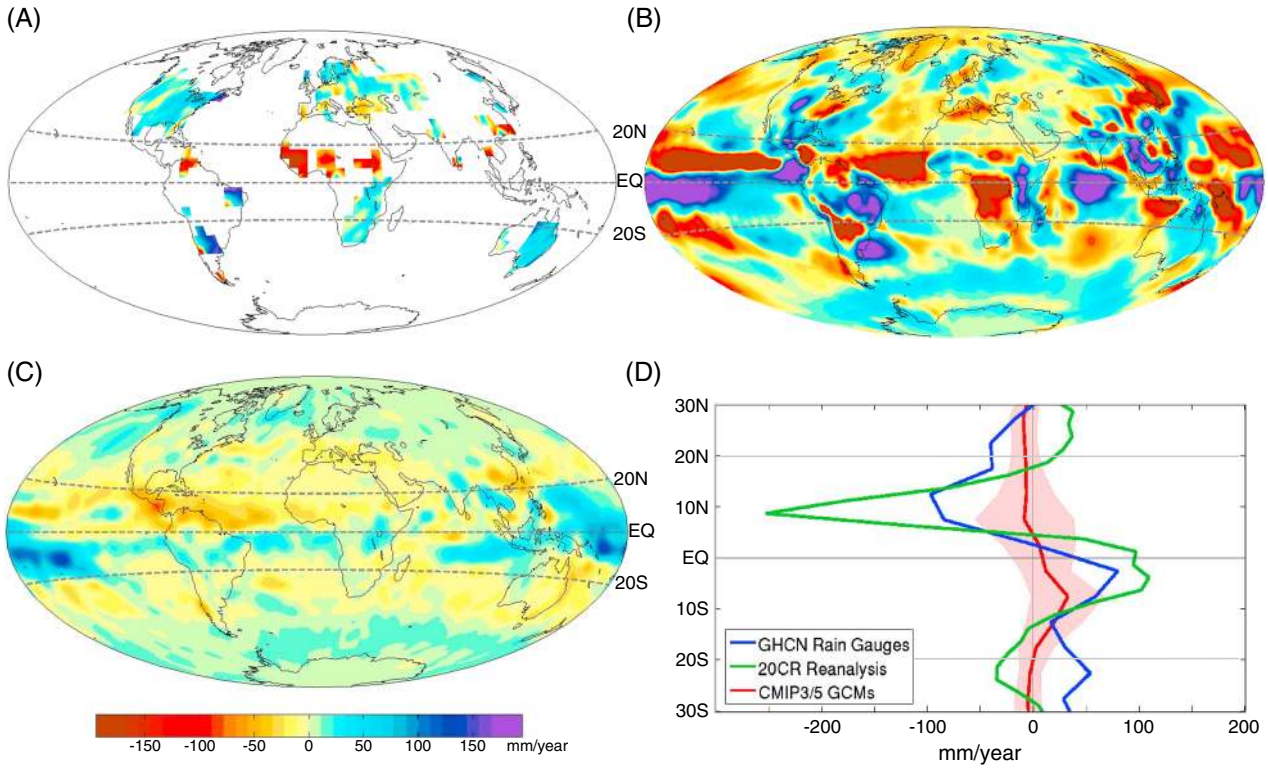

Figure 2. Spatial map and zonal mean of changes in precipitation. Changes in precipitation from 1931–1950 to 1971–1990 based on (a) the Global Historical Climatology Network (GHCN) gridded products, (b) the 20th century reanalysis project (20CR), and (c) the ensemble mean of the 20th century climate historical simulations from 14 GCMs in CMIP3 and 12 GCMs from CMIP5. (d) The zonal mean of (a), (b), and (c). The red shading represents the spread of one standard deviation at each latitude among GCMs.

with more heating). With this framework, one would expect models with more cooling in the NH to have an increase in northward cross-equatorial atmospheric energy transport and a southward shift of tropical rain, and this can be seen in Figure 3a.

[9] Having shown that tropical precipitation shifts are highly anticorrelated with cross-equatorial energy transports, we next perform an attribution study to explain the cross-equatorial energy transport in each model. Here we list out the steps for our attribution analysis of tropical precipitation shift in GCMs:

[10] 1. We use the approximate partial radiative perturbation (APRP) [*Taylor et al.*, 2007] method to separate changes in shortwave (SW) radiation into changes due to variations in surface albedo, cloud, noncloud SW scattering, and noncloud SW absorption. Surface albedo includes changes in sea ice and snow cover. Cloud includes changes in cloud area and cloud properties. Noncloud shortwave scattering is the change in atmospheric scattering that cannot be explained by surface albedo or cloud and is primarily due to changes in scattering aerosols. Noncloud SW absorption is the change in atmospheric absorption that cannot be explained by surface albedo or cloud, which is primarily due to the changes in absorbing aerosols, ozone, and water vapor. The sum of the four terms is the same as the difference in net incoming shortwave radiation between 1931–1950 and 1971–1990. The APRP method is particularly accurate for this type of multimodel comparison study since it does not require considering the differences in model climatology. However, the one-layer atmosphere assumption only works for SW radiation.

[11] 2. We use the radiative kernel technique [*Soden et al.*, 2008] to calculate the changes in longwave radiation due to variations in cloud, lapse rate, water vapor, and surface temperature. This technique provides a simple way to partition changes in longwave radiation across different models using a consistent methodology. Cloud feedbacks cannot be evaluated directly from a cloud radiative kernel because of strong nonlinearities, but they can be estimated from the change in cloud forcing and the difference between the full-sky and clear-sky kernels. We also calculate a longwave residual term, which is the difference between the changes in longwave radiation and the sum of all terms.

[12] 3. Changes in surface flux also contribute to the atmospheric energy budget, and there are two factors that can cause changes in this: changes in ocean heat transport and differential ocean heat uptake. We can interpret changes in surface fluxes as due to variations in these aspects of the ocean, which can be due to either natural variability or aerosol- or global warming–induced trends.

[13] 4. We calculate the implied cross-equator energy transport change due to different terms (described in steps 1–3) by the equations below [*Frierson and Hwang*, 2012; *Wu et al.*, 2010; *Donohoe and Battisti*, 2012; *Zelinka and Hartmann*, 2012]:

$$F_A(\phi = 0) = \int_{-\frac{\pi}{2}}^{0} \int_{0}^{2\pi} Q_A a^2 \cos\phi \mathrm{d}\lambda \mathrm{d}\phi = -\int_{0}^{\frac{\pi}{2}} \int_{0}^{2\pi} Q_A a^2 \cos\phi \mathrm{d}\lambda \mathrm{d}\phi,$$

where $F_A(\phi = 0)$ is the implied cross-equator energy transport, ϕ is latitude, λ is longitude, a is radius of the Earth,

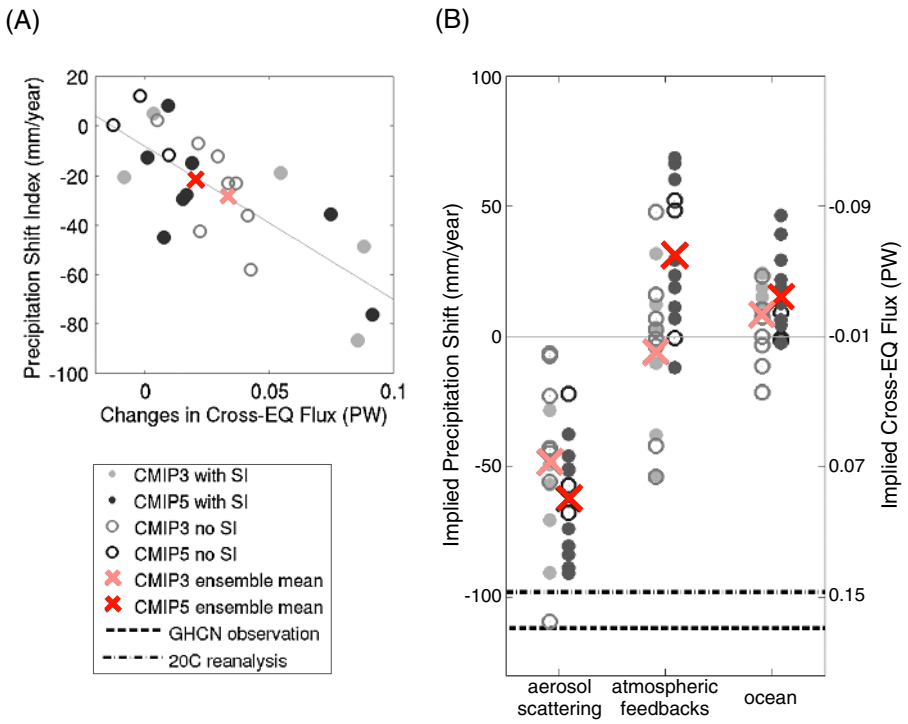

Figure 3. Attribution of tropical precipitation shift based on the global energetic framework. (a) The tropical precipitation shift (defined as changes in precipitation from equator to 20°N minus the changes from equator to 20°S) versus changes in cross-equatorial atmospheric energy transport. Grey circles are models from CMIP3. Black circles are models from CMIP5. Open circles indicate models with no indirect aerosol effects (no SI), closed circles indicate models with indirect aerosol effects (SI), and the red and the pink Xs indicate the ensemble means of the CMIP3 models and the CMIP5 models, respectively. The light grey solid line shows the best linear fit of all models. (B) Attribution of tropical precipitation shift and changes in cross-EQ transport. The black dashed and black dashed-dotted lines mark the precipitation shifts in GHCN and 20CR, respectively.

and Q_A is the change in atmospheric energy budget due to a factor described in steps (1)–(3) with its global mean value subtracted out. The results are plotted in Figure 3b (y axes on the right). In Figure 3b, we sum up all of the terms related with atmospheric radiative feedback, but we have also investigated their individual contributions (Supplementary Figure S5). For GCMs that simulate aerosol indirect effects, the indirect effect dominates the structure of shortwave cloud effects; therefore, we include the shortwave cloud effect into the scattering aerosol term in these models. However, even without including the indirect effect, scattering aerosols are still the most dominant term in multimodel mean (Supplementary Figure S5).

[14] 5. We estimate how much southward shift of precipitation may be induced by the implied cross-equator energy transport change due to each climate component (Figure 3b, y axis on the left) using the linear relationship in Figure 3a.

4. Aerosol Forcings and Tropical Precipitation

[15] One possible cause of the southward precipitation shift from 1931–1950 to 1971–1990 is scattering aerosol-induced cooling that primarily occurs in the NH. The 1971–1990 time period experienced the most dramatic southward shift (Figure 1) and is also the time period that sulfate aerosols emissions peaked. Because aerosols have short lifetimes of a week or two, they are concentrated close to their sources primarily in the NH extratropics and thus cool the NH relative to the Southern Hemisphere (SH). The notion that differential radiative forcings due to reflecting aerosols can shift tropical precipitation southward has been emphasized previously [*Chang et al.*, 2010; *Biasutti and Giannini*, 2006] and has been demonstrated in single-model or single-forcing experiments [*Rotstayn et al.*, 2000; *Williams et al.*, 2001; *Rotstayn and Lohmann*, 2002; *Held et al.*, 2005; *Yoshimori and Broccoli*, 2008; *Bollasina et al.*, 2011]. The method described in the last section allows us to address the role of aerosols, ocean processes, and climate feedbacks quantitatively across a large suite of models.

[16] Scattering aerosol (Figure 3b) is the dominant term in the multimodel mean, which indicates that this term is the main cause of the northward cross-equatorial energy transport and the southward precipitation shift. Other terms (Figures 3b and S5), such as longwave cloud effects, water vapor greenhouse effect, and ocean heat uptake and circulation changes can influence cross-equatorial transport as well. In some models, these are the dominant terms. However, the hemispheric asymmetries of these terms are not consistent across GCMs, introducing a northward shift in some GCMs, but a shift of opposite sign in others. The spread across GCMs could be due to the differences in natural variability or uncertainties in climate feedbacks with global warming.

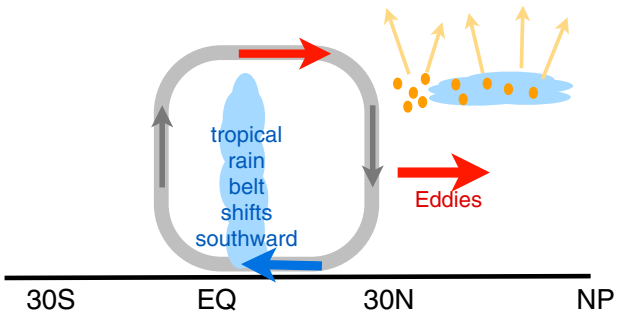

Figure 4. Schematic of the proposed mechanism for the southward tropical precipitation shift. Sulfate aerosols are primarily located in Northern Hemisphere midlatitudes during 1971–1990. Aerosol direct and indirect effects decrease the absorbed solar radiation and induce a strong cooling locally. This cooling is spread into the Northern Hemisphere tropics by baroclinic eddies. An anomalous Hadley circulation is induced in order to transport energy from the Southern Hemisphere to the Northern Hemisphere and keep the tropospheric temperature gradients relatively flat within the tropics. Since most of the water vapor is in the lower troposphere, this anomalous Hadley circulation transports an anomalous southward moisture flow and results in a southward shift of the tropical rain belt.

5. Conclusions and Discussions

[17] These results suggest that scattering aerosols are the primary driver of the multimodel mean tendency to shift precipitation southward in the late 20th century (Figure 4, mechanism described), and aerosols lead to much of the model-to-model variability in the simulated shifts as well. One might infer that since all models underestimate the observed precipitation shift (Figure 3b, black dashed and black dashed-dotted lines), more aerosol forcing should be added to the models to improve agreement with observations. However, other energetic responses in the atmosphere and ocean changes (Figure 3b) also lead to significant model-to-model spread in the simulations. The important role of processes such as clouds, surface albedo, and the ocean, along with observational uncertainties in the historical precipitation data set imply that this likely will not be useful as an observational constraint on past aerosol effects.

[18] Another factor that may explain the underestimation of the southward shift in GCMs is that GCMs fail to simulate the historical variations in oceanic circulation. A weakening in the thermohaline circulation has been proposed to explain the variation in the interhemispheric thermal anomaly, which is tightly linked with tropical precipitation [*Baines and Folland*, 2007; *Thompson et al.*, 2010; *Friedman et al.*, 2013]. However, it is unclear if the variation in ocean is due primarily to natural variability or anthropogenic forcings. *Booth et al.* [2012] proposed that aerosols may be the driver of the observed oceanic variability in North Atlantic during the 20th century, although their results are highly model dependent [*Chiang et al.*, 2013]. It is also possible that GCMs simulate too little shift for a given forcing. However, the fact remains that large fraction of the southward shift of tropical precipitation in the late 20th century was likely driven by scattering aerosol emissions.

[19] After clean air legislation was enacted in the United States and Europe in the early 1990s, scattering aerosol concentrations were reduced significantly. In the 21st century, scattering aerosols are expected to continue to decrease, although this assumes continued strict controls on sulfate emissions. One may expect that this would cause a continued northward recovery of tropical precipitation; however, changes in other energetic terms in the atmosphere and ocean responses can clearly complicate the story [*Friedman et al.*, 2013]. A better estimate of changes in the radiation budget and ocean circulation in the future will help narrow the uncertainties in our future projections of tropical precipitation.

[20] **Acknowledgments.** We acknowledge the World Climate Research Programme's Working Group on Coupled Modeling, which is responsible for CMIP, and we thank the climate modeling groups (listed in Figure S5 of this paper) for producing and making available their model output. For CMIP, the U.S. Department of Energy's Program for Climate Model Diagnosis and Intercomparison provides coordinating support and led the development of software infrastructure in partnership with the Global Organization for Earth System Science Portals Support for the Twentieth Century Reanalysis Project data set is provided by the U.S. Department of Energy, Office of Science Innovative and Novel Computational Impact on Theory and Experiment (DOE INCITE) program, and Office of Biological and Environmental Research (BER), and by the National Oceanic and Atmospheric Administration Climate Program Office. GPCC Precipitation data provided by the NOAA/OAR/ESRL PSD, Boulder, Colorado, USA, from their Web site at http://www.esrl.noaa.gov/psd/. We thank Chia Chou and an anonymous reviewer for their constructive comments, and J. M. Wallace, P. Arkin, Q. Fu and E. A. Barnes for improving earlier version of this manuscript. YTH and DMWF are supported by NSF grants AGS-0846641 and AGS-0936059. SMK was supported by the year 2011 Research Fund of the UNIST (Ulsan National Institute of Science and Technology).

[21] The Editor thanks Chia Chou and an anonymous reviewer for their assistance in evaluating this paper.

References

Baines, P. G., and C. K. Folland (2007), Evidence for a rapid global climate shift across the late 1960s, *J. Clim.*, *20*, 2721.

Biasutti, M., and A. Giannini (2006), Robust Sahel drying in response to late 20th century forcings, *Geophys. Res. Lett.*, *33*, L11706, doi:10.1029/2006GL026067.

Bollasina, M. A., Y. Ming, and V. Ramaswamy (2011), Anthropogenic aerosols and the weakening of South Asian summer monsoon, *Science*, *334*, 502–505.

Booth, B. B., N. J. Dunstone, P. R. Halloran, T. Andrews, and N. Bellouin (2012), Aerosols implicated as a prime driver of twentieth-century North Atlantic climate variability, *Nature*, *484*, 228–232.

Chang, C.-Y., J. C. H. Chiang, M. F. Wehner, A. R. Friedman, and R. Ruedy (2010), Sulfate aerosol control of Tropical Atlantic climate over the 20th century, *J. Clim.*, *24*, 2540–2555.

Chiang, J. C. H., and C. M. Bitz (2005), Influence of high latitude ice cover on the marine Intertropical Convergence Zone, *Clim. Dyn.*, *25*, 477–496.

Chiang, J. C. H., C.-Y. Chang, and M. F. Wehner (2013), Long-term trends of the Atlantic interhemispheric SST gradient in the CMIP5 historical simulations, in revision for *J. Clim.*.

Chung, C. E., and V. Ramanathan (2006), Weakening of North Indian SST gradients and the monsoon rainfall in India and the Sahel, *J. Clim.*, *19*, 2036–2045.

Compo, G. P. et al. (2011), The twentieth century reanalysis project, *Q. J. R. Meteorol. Soc.*, *137*, 1–28.

Dai, A. et al. (2004), The recent Sahel drought is real, *Int. J. Climatol.*, *24*, 1323–1331.

Donohoe, A., and D. S. Battisti (2012), What determines meridional heat transport in climate models?, *J. Clim.*, *25*, 3832–3850.

Folland, C. K., T. N. Palmer, and D. E. Parker (1986), Sahel Rainfall and worldwide sea temperatures, 1901–85, *Nature*, *320*, 602–607.

Friedman, A. R., Y.-T. Hwang, J. C. H. Chiang, and D. M. W. Frierson (2013), The interhemispheric temperature asymmetry over the 20th century and in future projections, *J. Clim.*, in press.

Frierson, D. M. W., and Y.-T. Hwang (2012), Extratropical influence on ITCZ shifts in slab ocean simulation of global warming, *J. Clim.*, *25*, 720–733.

Giannini, A., R. Saravanan, and P. Chang (2003), Oceanic forcing of Sahel rainfall on interannual to interdecadal time scales, *Science*, *302*, 1027–1030.

Held, I. M., T. L. Delworth, J. Lu, K. L. Findell, and T. R. Knutson (2005), Simulation of Sahel drought in the 20th and 21st centuries, *Proc. Natl. Acad. Sci. U. S. A.*, *102*, 17891–17896.

Hwang, Y.-T., and D. M. W. Frierson (2013), Link between the double intertropical convergence zone problem and cloud biases over the Southern Ocean, *Proc. Natl. Acad. Sci. U. S. A.* early online release, doi:10.1073/pnas. 121302110.

Kang, S. M., I. M. Held, D. M. W. Frierson, and M. Zhao (2008), The response of the ITCZ to extratropical thermal forcing: Idealized slab-ocean experiments with a GCM, *J. Clim.*, *21*, 3521–3532.

Kang, S. M., D. M. W. Frierson, and I. M. Held (2009), The tropical response to extratropical thermal forcing in an idealized GCM: The importance of radiative feedbacks and convective parameterization, *J. Atmos. Sci.*, *66*, 2812–2827.

Knight, J. R., R. J. Allan, C. K. Folland, M. Vellinga, and M. E. Mann (2005), A signature of persistent natural thermohaline circulation cycles in observed climate, *Geophys. Res. Lett.*, *32*, L20708, doi:10.1029/2005GL024233.

Lin, J.-L. (2007), The double-ITCZ problem in IPCC AR4 coupled GCMs: Ocean-atmosphere feedback analysis, *J. Clim.*, *20*, 4497–4525.

Mitchell, T. D., and P. D. Jones (2005), An improved method of constructing a database of monthly climate observations and associated high-resolution grids, *Int. J. Climatol.*, *6*, 693–712.

Nicholson, S. E. (1993), An overview of African rainfall fluctuations of the last decade, *J. Clim.*, *6*, 1463–1466.

Peterson, T. C., and R. S. Vose (1997), An overview of the global historical climatology network temperature data base, *Bull. Am. Meteorol. Soc.*, *78*, 2837–2849.

Rotstayn, L. D., and U. Lohmann (2002), Tropical rainfall trends and the indirect aerosol effect, *J. Clim.*, *15*, 2103–2116.

Rotstayn, L. D., B. F. Ryan, and J. E. Penner (2000), Precipitation changes in a GCM resulting from the indirect effects of anthropogenic aerosols, *Geophys. Res. Lett.*, *27*, 3045–3048.

Schneider, U., A. Becker, P. Finger, A. Meyer-Christoffer, M. Ziese, and B. Rudolf (2013), GPCC's new land surface precipitation climatology based on quality-controlled in situ data and its role in quantifying the global water cycle, *Theor. Appl. Climatol.*, 1–26.

Smith, S. J., J. Van Aardenne, Z. Klimont, R. J. Andres, A. Volke, and S. Delgado Arias (2011), Anthropogenic sulfur dioxide emissions: 1850-2005, *Atmos. Chem. Phys.*, *11*(3) 1101-1116.

Soden, B. J. et al. (2008), Quantifying climate feedbacks using radiative kernels, *J. Clim.*, *21*, 3504–3520.

Solomon, S., et al. (2007), *Climate Change 2007: The Physical Science Basis*, 996 pp., Cambridge Univ. Press, Cambridge, United Kingdom and New York, NY, USA.

Taylor, K. E. et al. (2007), Estimating shortwave radiative forcing and response in climate models, *J. Clim.*, *20*, 2530–2543.

Tett, S. F. B., et al. (2002), Estimation of natural and anthropogenic contributions to twentieth century temperature change, *J. Geophys. Res.*, *107*(D16), 4306, doi:10.1029/2000JD000028.

Thompson, D. W. J., J. M. Wallace, J. J. Kennedy, and P. D. Jones (2010), An abrupt drop in Northern Hemisphere sea surface temperature around 1970, *Nature*, *467*, 444–447.

Williams, K. D., A. Jones, D. L. Roberts, C. A. Senior, and M. J. Woodage (2001), The response of the climate system to the indirect effects of anthropogenic sulfate aerosol, *Clim. Dyn.*, *17*, 845–856.

Wu, Y., M. Ting, R. Seager, H.-P. Huang, and M. A. Cane (2010), Changes in storm tracks and energy transports in a warmer climate simulated by the GFDL CM2.1 model, *Clim. Dyn.*, *37*, 53–72.

Yoshimori, M., and A. J. Broccoli (2008), Equilibrium response of an atmosphere-mixed layer ocean model to different radiative forcing agents: global and zonal mean response, *J. Climate*, *21*, 4399–4423.

Zelinka, M. D., and D. L. Hartmann (2012), Climate feedbacks and their implications for poleward energy flux changes in a warming climate, *J. Clim.*, *25*, 608–624.

Zhang, R., and T. L. Delworth (2005), Simulated tropical response to a substantial weakening of the Atlantic thermohaline circulation, *J. Clim.*, *18*, 1853–1860.

Zhang, R., and T. L. Delworth (2006), Impact of Atlantic multidecadal oscillations on India/Sahel rainfall and Atlantic hurricanes, *Geophys. Res. Lett.*, *33*, L17712, doi:10.1029/2006GL026267.